

A Predictive Semiclassical Model for Coherent and Incoherent Emission in the Strong Field Regime: The Mollow Triplet Revisited

Hsing-Ta Chen,^{1,*} Tao E. Li,¹ Abraham Nitzan,¹ and Joseph E. Subotnik¹

¹*Department of Chemistry, University of Pennsylvania,
Philadelphia, Pennsylvania 19104, U.S.A.*

Abstract

We re-investigate the famous Mollow triplet and show that most of the well-known quantum characteristics of the Mollow triplet—including incoherent emission and a non-standard dependence of the sidebands on detuning—can be recovered quantitatively using semiclassical dynamics with a classical light field. In fact, by not relying on the rotating wave approximation, a semiclassical model predicts some quantum effects beyond the quantum optical Bloch equation, including higher order scattering and asymmetric sideband features. This letter highlights the fact that, with strong intensities, many putatively quantum features of light–matter interactions arise from a simple balance of mean-field electrodynamics and elementary spontaneous emission which requires minimal computational cost. Our results suggest that the application of semiclassical electrodynamics to problems with strong light–matter coupling in the fields of nanophotonics and superradiance are likely to yield a plethora of new information.

* hsingc@sas.upenn.edu

Light-matter interactions are interesting for two reasons: 1. Light scattered from matter carries detailed information about the matter itself; 2. Generating quantum light sources and entangled light-matter states is crucial for novel applications in quantum technology. For example, via light-matter interactions, a beam of classical light (a coherent laser) can be transformed into non-classical light (photons) with quantum features, such as fluctuations and cascade emission. In this letter, we will focus on one of the simplest examples of matter interacting with a strong light field: a two-level system (TLS) strongly driven by a monochromatic light. For such a case, it is well known that the TLS will emit light with a frequency spectrum composed of three peaks, known as a *Mollow triplet*[1, 2].

The Mollow triplet spectrum is a universal signature of a quantum system undergoing resonance fluorescence and cannot be explained by classical optics: the prediction of the Mollow triplet spectrum is one of the key achievement of *quantum* optics. The salient features of the Mollow triplet are as follows. First, the spectrum is composed of one central peak at the driving frequency and two sidebands shifted from the central peak by the Rabi frequency[3–6]. Second, at resonance, the fluorescence triplet is dominated by incoherent emission[2, 7–9]. Third, a radiative cascade leads to photon antibunching and blinking[10–14]. These three universal quantum optical features have been demonstrated in (artificial) atomic system[15–19], quantum dots[20–27], and nitrogen vacancy defects[28].

To understand the features above, the usual approach in quantum optics is to propagate the quantum optical Bloch equation (OBE), and then infer the scattered field from the correlation function of the matter using quantum electrodynamics (QED)[29–31]. More precisely, one makes an independent process assumption[30]: the TLS responds to the incident field (a single, highly occupied photon mode) and relaxes as the radiation field (a reservoir of unoccupied photon modes) gains population by fluorescence. The propagation of the quantum OBE usually relies on the rotating wave approximation (RWA), which is valid near resonance and allows for analytical expressions[7].

In this letter, we show that, quite surprisingly, most of the quantum features of the Mollow triplet can be captured by semiclassical simulations without relying on the RWA. In fact, a semiclassical model can predict some quantum effects beyond what is possible with the OBE and the RWA, such as higher order sidebands and an asymmetric spectrum. Furthermore, because classical electrodynamics is so inexpensive, the methods discussed below should be applicable to large systems in environments with arbitrary dielectrics where a rigorous

quantum treatment is not feasible nowadays.

Driven Quantum System To simulate the features of the Mollow triplet, we consider a TLS driven by a single-mode laser field in an effectively 1D space. The electronic TLS Hamiltonian is $\hat{H}_S = \hbar\omega_0 |1\rangle\langle 1|$ where the ground state $|0\rangle$ and the excited state $|1\rangle$ are separated by an energy difference $\hbar\omega_0$. The transition dipole moment operator is given by $\hat{\mathcal{P}}(x) = \mathbf{d}(x)(|0\rangle\langle 1| + |1\rangle\langle 0|)$. Here, for simplicity, we assume that the polarization distribution takes the form of $\mathbf{d}(x) = \mu\sqrt{\frac{a}{\pi}}e^{-ax^2}\mathbf{e}_z$ and has a uniform charge distributions in the yz plane. We also assume that the width of the polarization distribution ($\sigma = 1/\sqrt{2a}$) is chosen to be relatively small in space so that the long-wavelength approximation is valid. The quantum state of the TLS is described by either the electronic density matrix $\hat{\rho}$ or an ensemble of electronic wavefunctions $\{|\psi^\ell\rangle\}$.

For this semiclassical model, both the incident laser photons and the scattered field are treated as classical electromagnetic (EM) fields. We assume that the incident laser photons are in a coherent state, so that the average field observables closely resemble a continuous wave (CW) EM field. Thus, for simplicity, the incident EM field takes the form: $\mathbf{E}_L(x, t) = \frac{A_L}{\sqrt{\epsilon_0}} \cos \omega_L \left(\frac{x}{c} - t\right) \mathbf{e}_z$ and $\mathbf{B}_L(x, t) = -\sqrt{\mu_0}A_L \cos \omega_L \left(\frac{x}{c} - t\right) \mathbf{e}_y$ where A_L is the amplitude and ω_L is the frequency of the incident laser field. As $\sigma \rightarrow 0$, the driving term can be approximated by $-\int dx \mathbf{E}_L(x, t) \cdot \mathbf{d}(x) \approx \hbar\Omega_r \cos(\omega_L t)$ where $\Omega_r = -\mu A_L/\hbar$ is the Rabi frequency. The CW fields \mathbf{E}_L and \mathbf{B}_L satisfy source-less Maxwell equations: $\frac{\partial}{\partial t} \mathbf{B}_L = -\nabla \times \mathbf{E}_L$, $\frac{\partial}{\partial t} \mathbf{E}_L = c^2 \nabla \times \mathbf{B}_L$. In other words, the CW fields constitute standalone external fields driving the TLS. Let us now describe how we model the dynamics of the TLS state plus the scattered EM fields.

Ehrenfest+R Dynamics for Driven TLS To model the Mollow triplet, we use “Ehrenfest+R” dynamics—a simple amended version of Ehrenfest dynamics to account for spontaneous emission[32]. In the context of a driven TLS, the fundamental variables for Ehrenfest+R dynamics are the same as those for Ehrenfest dynamics: $\{c_0^\ell, c_1^\ell, \mathbf{E}_S^\ell, \mathbf{B}_S^\ell\}$ where we use ℓ to index each trajectory. Recall that the coupled equations of motion for Ehrenfest

dynamics are of the standard Maxwell–Schrodinger form:

$$\frac{\partial}{\partial t} c_0^\ell(t) = \frac{i}{\hbar} H_{01}(t) c_1^\ell(t), \quad (1a)$$

$$\frac{\partial}{\partial t} c_1^\ell(t) = -i\omega_0 c_1^\ell(t) + \frac{i}{\hbar} H_{01}(t) c_0^\ell(t), \quad (1b)$$

$$\frac{\partial}{\partial t} \mathbf{E}_S^\ell(x, t) = c^2 \nabla \times \mathbf{B}_S^\ell(x, t) - \frac{1}{\epsilon_0} \mathbf{J}^\ell(x, t), \quad (1c)$$

$$\frac{\partial}{\partial t} \mathbf{B}_S^\ell(x, t) = -\nabla \times \mathbf{E}_S^\ell(x, t). \quad (1d)$$

Here, the scattered field is an ensemble of classical EM field $\{\mathbf{E}_S^\ell, \mathbf{B}_S^\ell\}$ with the initial condition in the vacuum (i.e. $\mathbf{E}_S^\ell(x, 0) = \mathbf{B}_S^\ell(x, 0) = 0$). The average current generated by the TLS is $\mathbf{J}^\ell(x, t) = -2\omega_0 c_0^\ell(t) c_1^\ell(t)^* \mathbf{d}(x)$. In Eq. (1), note that we work with the wavefunction of the electronic system, $|\psi^\ell\rangle = c_0^\ell |0\rangle + c_1^\ell |1\rangle$, and we can build the electronic density matrix as $\rho_{ij} = \frac{1}{N} \sum_\ell c_i^\ell c_j^{\ell*}$ for N trajectories. The electric dipole coupling is $H_{01}(t) = \int_{-\infty}^{\infty} dx [\mathbf{E}_L(x, t) + \mathbf{E}_S^\ell(x, t)] \cdot \mathbf{d}(x)$, which is composed of the laser driving term (coupled to the laser field \mathbf{E}_L) and the radiation self-interaction term (coupled to the scattered field \mathbf{E}_S^ℓ).

While Eq. (1a)–(1d) constitute Ehrenfest dynamics, the augmentations needed for the “+R” correction are threefold: 1. population relaxation, 2. stochastic dephasing, and 3. EM field rescaling.

1. *Population relaxation.* Note that Ehrenfest dynamics do not fully include spontaneous emission[33]. To recover spontaneous emission, we add population relaxation after every time step dt propagating Eq. (1), and adjust the electronic wave function by

$$c_0^\ell \rightarrow \frac{c_0^\ell}{|c_0^\ell|} \sqrt{|c_0^\ell|^2 + k_R |c_1^\ell|^2} dt, \quad (2a)$$

$$c_1^\ell \rightarrow \frac{c_1^\ell}{|c_1^\ell|} \sqrt{|c_1^\ell|^2 - k_R |c_0^\ell|^2} dt. \quad (2b)$$

Here, $k_R \equiv 2\kappa |c_1^\ell|^2 \text{Im} [e^{i\phi_\ell} c_0^\ell c_1^{\ell*} / |c_0^\ell c_1^{\ell*}|]^2$ is the +R relaxation rate ($k_R = 0$ if $\rho_{11} = 0$) and $\kappa = \mu^2 \omega_0 / \hbar \epsilon_0 c$ is the Fermi’s golden rule (FGR) rate for 1D space. $\phi_\ell \in [0, 2\pi]$ is a random phase chosen at the beginning of each trajectory.

2. *Stochastic dephasing.* After each time step, we implement dephasing by multiplication with another random phase $\Phi \in [0, 2\pi]$:

$$c_0^\ell \rightarrow c_0^\ell e^{i\Phi} \text{ if } \text{RN} < \kappa |c_1^\ell|^2 dt \quad (3)$$

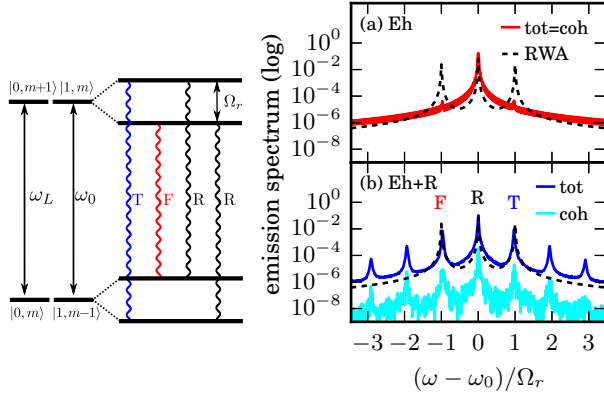


Figure 1. (Left) Energy diagram at resonance ($\omega_L = \omega_0$) according to a quantum dressed state representation. The ground state combined with $m + 1$ incident photons $|0, m + 1\rangle$ aligns energetically with the excited state combined with m photons $|1, m\rangle$ for all $m > 0$. After diagonalization, two dressed states are separated by the Rabi frequency $|\Omega_r|$. The radiative transitions among the dressed states are denoted as: Rayleigh emission ($\Omega_R = \omega_L$, labeled R in black), fluorescence emission ($\Omega_F = \omega_L - \Omega_r$, labeled F in red), and three-photon emission ($\Omega_T = \omega_L + \Omega_r$, labeled T in blue). (Right) Semi-log plot of the scattering spectra of the driven TLS as obtained by (a) Ehrenfest and (b) Ehrenfest+R dynamics. The black dashed line is the analytical result given by the quantum OBE within the RWA. The Ehrenfest dynamics (colored red) yield only coherent emission and that emission is restricted to the incident laser frequency. By contrast, for Ehrenfest+R dynamics, we find both the coherent emission $|\langle \mathbf{E}_S(\omega) \rangle|^2$ (colored cyan) and the total emission spectrum $\langle |\mathbf{E}_S(\omega)|^2 \rangle$ (colored blue). Note that the Ehrenfest+R dynamics predict higher order emission peaks at $\omega - \omega_0 = \pm 2\Omega_r, \pm 3\Omega_r, \dots$.

where $\text{RN} \in [0, 1]$ is a random number.

3. *EM field rescaling.* In order to conserve energy, after every population relaxation event in Eq. (2), we rescale the scattered EM field by

$$\mathbf{E}_S^\ell \rightarrow \mathbf{E}_S^\ell + \alpha^\ell \delta \mathbf{E}_S, \quad (4a)$$

$$\mathbf{B}_S^\ell \rightarrow \mathbf{B}_S^\ell + \beta^\ell \delta \mathbf{B}_S. \quad (4b)$$

Here, the rescaling fields are chosen to be $\delta \mathbf{E}_S(x) = -\mu \sqrt{\frac{a}{\pi}} 4a^2 x^2 e^{-ax^2} \mathbf{e}_z$ and $\delta \mathbf{B}_S(x) = \mu \sqrt{\frac{a}{\pi}} \frac{4}{3} a^2 x^3 e^{-ax^2} \mathbf{e}_y$, which depend on the polarization distribution \mathbf{d} only. The coefficients

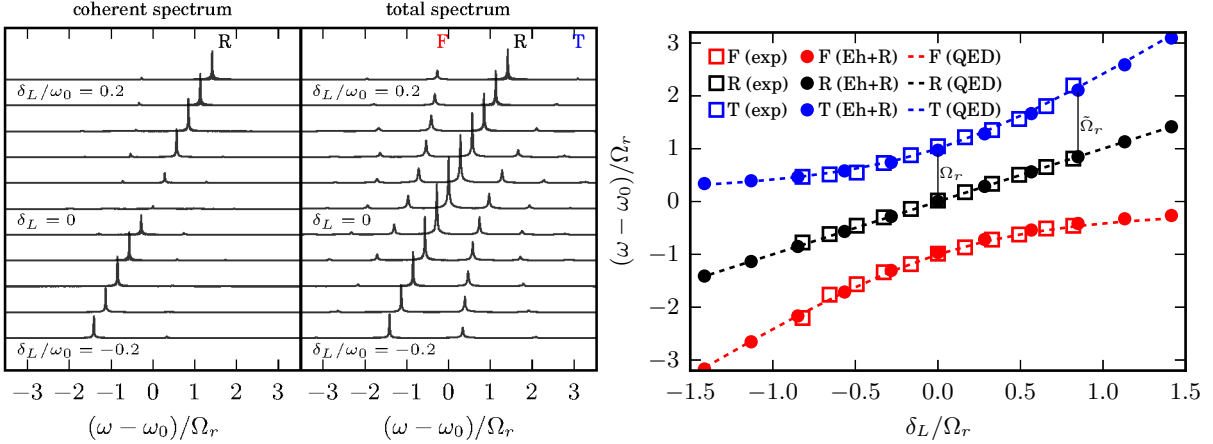


Figure 2. (a) Total scattering spectra of the driven TLS when varying the laser detuning δ_L . We plot both the coherent scattering spectrum $|\langle \mathbf{E}_S(\omega) \rangle|^2$ (left) and the total intensity spectrum $\langle |\mathbf{E}_S(\omega)|^2 \rangle$ (right) as obtained by the Ehrenfest+R dynamics. Note that coherent emission occurs only at the Rayleigh emission ($\omega = \omega_L$) and vanishes at resonance ($\delta_L = 0$) for the case of a strong incident field ($\Omega_r \gg \kappa$)[39]. (b) We plot three peak positions as a function of the laser detuning for Rayleigh (colored black), fluorescence (colored red), and three-photon (colored blue). The dashed lines are the quantum results, i.e. $\Omega_R = \omega_L$, $\Omega_F = \omega_L - \tilde{\Omega}_r$, and $\Omega_T = \omega_L + \tilde{\Omega}_r$. The solid circles are the Ehrenfest+R data extracted from the left panel. The boxes are experimental data from Ref. 25. As a function of the detuning, Ehrenfest+R dynamics predict the correct peak positions in agreement with QED and experiment.

α^ℓ, β^ℓ can be calculated to be

$$\alpha^\ell = dt \sqrt{\frac{c\omega_0 k_R}{\Lambda \epsilon_0} \frac{|c_1^\ell|^2}{\int dv |\delta \mathbf{E}_S|^2} \text{sgn} \left(\text{Im} \left[c_0^\ell c_1^{\ell*} e^{i\phi^\ell} \right] \right)} \quad (5a)$$

$$\beta^\ell = dt \sqrt{\frac{c\omega_0 k_R}{\Lambda} \frac{\mu_0 |c_1^\ell|^2}{\int dv |\delta \mathbf{B}_S|^2} \text{sgn} \left(\text{Im} \left[c_0^\ell c_1^{\ell*} e^{i\phi^\ell} \right] \right)}. \quad (5b)$$

Note that, for a Gaussian polarization distribution in 1D, the self-interference length is determined by $\Lambda = \frac{2}{3} \sqrt{\frac{2\pi}{a}}$, and we use the random phase ϕ_ℓ in Eq. (5). Ref. [34] demonstrates that Eq. (2)–(5) conserve energy for a ensemble of trajectories.

Finally, all together, the Ehrenfest+R dynamics are outlined in Eq. (1)–(5). One key motivation for Ehrenfest+R dynamics was the drive to distinguish the coherent emission ($\langle |\mathbf{E}_S|^2 \rangle$) from the total emission intensity ($\langle \mathbf{E}_S^2 \rangle$). This distinction is achieved by averaging over

an ensemble of trajectories, which has been very successful in the area of electron–nuclear dynamics, including surface hopping[35] and multiple spawning[36]. Importantly, the computational cost of running several Ehrenfest+R trajectories is moderate and easy to parallelize, such that simulating a large network of quantum emitters or an environment with complicated dielectrics should be possible in the future.

Mollow Triplet Spectrum The Mollow triplet arises when the FGR rate is much smaller than the Rabi frequency which is in turn smaller than the energy spacing of the TLS, i.e. $\kappa \ll \Omega_r \ll \omega_0$. For this reason, we choose parameters as follows: $\kappa/\omega_0 = 1/800$ and $\Omega_r/\omega_0 = 1/7$. The laser detuning between the incident laser field frequency and the TLS emission frequency is denoted as $\delta_L = \omega_L - \omega_0$. We assume that the initial state of the TLS is the ground state and uncoupled to the EM field, and the entire system reaches steady state at long times, which is independent from the initial condition.

We first focus on the *resonant* Mollow triplet ($\delta_L = 0$). In Fig. 1(a)–(b), we plot results from Ehrenfest dynamics and Ehrenfest+R dynamics. We find that Ehrenfest+R dynamics predict a resonant Mollow triplet spectrum at the correct three frequencies and the emission is predominantly incoherent as expected from QED. By contrast, without the +R correction, Ehrenfest dynamics produce only Rayleigh emission (i.e. only one frequency), and the emission is entirely coherent. To explain this behavior, we recall that the standard Ehrenfest approach can recover the correct spontaneous emission rate only when the quantum subsystem is mostly in the ground state[33, 37]. In the presence of the strong driving field, however, the TLS quantum system is almost always above saturation and oscillating between the ground and excited state, so that the standard Ehrenfest dynamics cannot emit the radiation field correctly. This result highlights the importance of spontaneous emission and stochastic dephasing as far as recovering key features of QED. As far as characterizing the Mollow triplet, Ehrenfest dynamics are not enough, but Ehrenfest+R dynamics appear sufficient.

With this promising result in mind, we now turn our attention to the Mollow triplet spectroscopy at varying incident field frequencies (non-zero detuning). From the energy diagram of QED, when the incident laser is off-resonant ($\delta_L \neq 0$), we expect that the Rayleigh scattering frequency changes linearly with respect to the laser detuning ($\Omega_R = \omega_L = \omega_0 + \delta_L$) and the separation of the sidebands increases following the generalized Rabi frequency, $\tilde{\Omega}_r = \sqrt{\Omega_r^2 + \delta_L^2}$, so that $\Omega_T = \omega_L + \tilde{\Omega}_r$ and $\Omega_F = \omega_L - \tilde{\Omega}_r$. In Fig. 2, we plot both the

coherent spectrum ($|\langle \mathbf{E}_S(\omega) \rangle|^2$) and the total intensity spectrum from Ehrenfest+R dynamics and extract the peak positions as a function of the laser detuning. We show conclusively that the Ehrenfest+R dynamics produce an accurate detuning dependence for the Mollow triplet peak positions in agreement with QED and experimental results[22, 25, 26, 38]. Interestingly, as opposed to the QED data (which is based on the quantum OBE with the RWA), the Ehrenfest+R dynamics (which go beyond the RWA) predict higher order emission sidebands ($\omega_L \pm n\tilde{\Omega}_r$) for $n = 2, 3, \dots$ (see Fig. 1(b)).

Next, let us compare the coherent emission and the total intensity. In Fig. 2, one can observe that the EM fields emitted by Ehrenfest+R dynamics are coherent only at the Rayleigh frequency ($\Omega_R = \omega_L$) and the sidebands are almost always incoherent.[39] Furthermore, the fraction of the coherent component at the Rayleigh frequency strongly depends on the laser detuning and will be suppressed when the laser frequency is at resonance. To quantify these observations, in Fig. 3(a), we plot the coherence fraction $|\langle \mathbf{E}_S(\omega) \rangle|^2 / \langle |\mathbf{E}_S(\omega)|^2 \rangle$ for the Rayleigh peak as a function of the laser detuning and compare against QED results[30]. To rationalize the detuning dependence of the coherence fraction, we recall that the spontaneous emission of a TLS quantum emitter on the excited state is dominated by incoherent emission[32]. Thus, when at resonance, the quantum emitter will be pumped to the excited state by the incident laser so that, after emission, all scattered light will be almost exclusively incoherent. By contrast, when the laser frequency is largely off-resonant, the quantum emitter will mostly stay near the ground state, so that coherent emission will dominate.

Finally, we focus on the sidebands of Mollow triplet. In Fig. 3(b), we plot the sideband ratio for the fluorescence peak, $\langle |\mathbf{E}_S(\Omega_F)|^2 \rangle / (\langle |\mathbf{E}_S(\Omega_F)|^2 \rangle + \langle |\mathbf{E}_S(\Omega_T)|^2 \rangle)$, as a function of the laser detuning. As is clear from the figure, Ehrenfest+R dynamics produce asymmetric sideband ratios, namely the F peak is higher than the T peak when the incident laser has a positive detuning ($\delta_L > 0$) and vice versa. In fact, the Ehrenfest+R model predicts a sideband ratio in near quantitative agreement with experimental measurements[22, 26]. By contrast, the RWA result incorrectly predicts a symmetric Mollow triplet spectrum for all δ_L , which reminds us that the RWA is valid only near resonance. The fact that the Ehrenfest+R dynamics can capture asymmetric sidebands indicates that contributions from the non-RWA terms (such as off-resonance and higher order[40–43]) are effectively included in this semi-classical model.

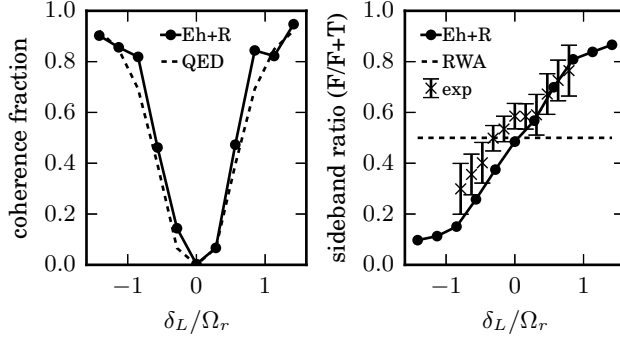


Figure 3. (a) The coherence fraction of the scattering intensity at the Rayleigh frequency ($\omega = \Omega_R$) as a function of the laser detuning. The circles are the Ehrenfest+R results and the dash line is the analytical result $|\langle \mathbf{E}_S(\Omega_R) \rangle|^2 / |\langle \mathbf{E}_S(\Omega_R) \rangle|^2 = 4\delta_L^2 (\Omega_r^2 + \delta_L^2) / (\Omega_r^2 + 2\delta_L^2)^2$. Note that the Rayleigh scattering signal is dominated by incoherent scattering when the incident laser is on resonance ($\delta_L = 0$) and becomes more coherent when off-resonant. (b) The relative sideband intensity for the fluorescence signal (denoted as $F/(F+T)$) as a function of the detuning. Note that the Ehrenfest+R results agree closely with the experimental data (adapted from Ref. 26). By contrast, the RWA always predicts (incorrectly) a symmetric Mollow triplet with $F/(F+T) = 0.5$.

Discussion and Conclusions In this letter, we have shown that, quite surprisingly, the key universal features of the Mollow triplet can be modeled with mixed quantum-classical theory and not just QED: we require only quantum matter plus classical light. The basic idea is that Ehrenfest+R dynamics incorporate both electronic self-interaction (as caused by explicit propagation of the scattered EM field) as well some of the quantum fluctuations of light (as caused by enforcing stochastic relaxation and dephasing). Furthermore, we have shown that because this method does not rely on the RWA, Ehrenfest+R can recover the correct scattering spectrum in a wide range of laser detuning far away from resonance, which is not possible with the usual QBE within the RWA.

Looking forward, on the one hand, even though we find accurate results with a semi-classical model, one should be cautious about extrapolating our results and rushing into judgment as to what is quantum and what is classical[44]. As a precaution, we note that the semiclassical model above cannot describe some quantum effects of the Mollow triplet that involve higher-order correlations, such as radiative cascaded emission and photon antibunching. On the other hand, it will be interesting to find out exactly how far this (or a similar) semiclassical model of light-matter interactions can take us. The success of the

Ehrenfest+R dynamics in recovering the Mollow triplet quantitatively is evidence that, with energy conservation, several nuanced features of quantum optics can be dissected classically. Just as a host of semiclassical non-adiabatic dynamics algorithms have transformed the field of photochemistry and molecular electronics over the past 20 years[45–48], our hope is that, with new semiclassical approaches for light–matter interactions, one will soon be able to realistically model many exciting new collective phenomena, including resonant energy transfer[37, 49], superradiance[50–52], cavity effects[53–55], and nanoplasmonics[56]. Further work in this regard will certainly be very exciting.

Acknowledgment This material is based upon work supported by the U.S. Department of Energy, Office of Science, Office of Basic Energy Sciences under Award Number DE-SC0019397. The research of AN is supported by the Israel-U.S. Binational Science Foundation. The authors thank Simone Luca Portalupi and Peter Michler for providing experimental data.

- [1] M. C. Newstein, Physical Review **167**, 89 (1968).
- [2] B. R. Mollow, Phys. Rev. **188**, 1969 (1969).
- [3] H. J. Kimble and L. Mandel, Physical Review A **13**, 2123 (1976).
- [4] E. del Valle and F. P. Laussy, Physical Review Letters **105** (2010), 10.1103/PhysRevLett.105.233601.
- [5] A. Moelbjerg, P. Kaer, M. Lorke, and J. Mørk, Physical Review Letters **108** (2012), 10.1103/PhysRevLett.108.017401.
- [6] D. P. S. McCutcheon and A. Nazir, Physical Review Letters **110** (2013), 10.1103/PhysRevLett.110.217401.
- [7] C. Cohen-Tannoudji and S. Reynaud, Journal of Physics B: Atomic and Molecular Physics **10**, 345 (1977).
- [8] S. Ates, S. M. Ulrich, S. Reitzenstein, A. Löffler, A. Forchel, and P. Michler, Physical Review Letters **103** (2009), 10.1103/PhysRevLett.103.167402.
- [9] S. Hughes and G. S. Agarwal, Physical Review Letters **118** (2017), 10.1103/PhysRevLett.118.063601.
- [10] A. Aspect, G. Roger, S. Reynaud, J. Dalibard, and C. Cohen-Tannoudji, Physical Review Letters **45**, 617 (1980).
- [11] C. A. Schrama, G. Nienhuis, H. A. Dijkerman, C. Steijsiger, and H. G. M. Heideman, Physical Review A **45**, 8045 (1992).
- [12] G. Nienhuis, Physical Review A **47**, 510 (1993).

[13] J. C. López Carreño, C. Sánchez Muñoz, D. Sanvitto, E. del Valle, and F. P. Laussy, Phys. Rev. Lett. **115**, 196402 (2015).

[14] H. J. Kimble, M. Dagenais, and L. Mandel, Phys. Rev. Lett. **39**, 691 (1977).

[15] F. Schudaf, C. R. S. Jr, and M. Hercher, J. Phys. B: At. Mol. Phys **7**, L198 (1974).

[16] F. Y. Wu, R. E. Grove, and S. Ezekiel, Physical Review Letters **35**, 1426 (1975).

[17] G. Wrigge, I. Gerhardt, J. Hwang, G. Zumofen, and V. Sandoghdar, Nature Physics **4**, 60 (2008).

[18] O. Astafiev, A. M. Zagoskin, A. A. Abdumalikov, Y. A. Pashkin, T. Yamamoto, K. Inomata, Y. Nakamura, and J. S. Tsai, Science **327**, 840 (2010).

[19] C. H. H. Schulte, J. Hansom, A. E. Jones, C. Matthiesen, C. Le Gall, and M. Atatüre, Nature **525**, 222 (2015).

[20] X. Xu, B. Sun, P. R. Berman, D. G. Steel, A. S. Bracker, D. Gammon, and L. J. Sham, Science **317**, 929 (2007).

[21] A. Muller, E. B. Flagg, P. Bianucci, X. Y. Wang, D. G. Deppe, W. Ma, J. Zhang, G. J. Salamo, M. Xiao, and C. K. Shih, Physical Review Letters **99** (2007), 10.1103/PhysRevLett.99.187402.

[22] A. Nick Vamivakas, Y. Zhao, C.-Y. Lu, and M. Atatüre, Nature Physics **5**, 198 (2009).

[23] E. B. Flagg, A. Muller, J. W. Robertson, S. Founta, D. G. Deppe, M. Xiao, W. Ma, G. J. Salamo, and C. K. Shih, Nature Physics **5**, 203 (2009).

[24] S. M. Ulrich, S. Ates, S. Reitzenstein, A. Löffler, A. Forchel, and P. Michler, Physical Review Letters **106** (2011), 10.1103/PhysRevLett.106.247402.

[25] A. Ulhaq, S. Weiler, S. M. Ulrich, R. Roßbach, M. Jetter, and P. Michler, Nature Photonics **6**, 238 (2012).

[26] A. Ulhaq, S. Weiler, C. Roy, S. M. Ulrich, M. Jetter, S. Hughes, and P. Michler, Optics Express **21**, 4382 (2013).

[27] K. G. Lagoudakis, K. A. Fischer, T. Sarmiento, P. L. McMahon, M. Radulaski, J. L. Zhang, Y. Kelaita, C. Dory, K. Müller, and J. Vučković, Physical Review Letters **118** (2017), 10.1103/PhysRevLett.118.013602.

[28] S. Rohr, E. Dupont-Ferrier, B. Pigeau, P. Verlot, V. Jacques, and O. Arcizet, Physical Review Letters **112** (2014), 10.1103/PhysRevLett.112.010502.

[29] C. Cohen-Tannoudji, J. Dupont-Roc, and G. Grynberg, *Photons and Atoms: Introduction to Quantum Electrodynamics* (Wiley, 1997).

[30] C. Cohen-Tannoudji, J. Dupont-Roc, and G. Grynberg, *Atom-Photon Interactions: Basic Processes and Applications* (Wiley-VCH, New York, 1998).

[31] A. Salam, *Molecular Quantum Electrodynamics: Long-Range Intermolecular Interactions* (John Wiley & Sons, Ltd, 2010).

[32] H.-T. Chen, T. E. Li, M. Sukharev, A. Nitzan, and J. E. Subotnik, arXiv:1806.04662 (2018).

[33] T. E. Li, A. Nitzan, M. Sukharev, T. Martinez, H.-T. Chen, and J. E. Subotnik, Phys. Rev. A **97**, 032105 (2018).

[34] T. E. Li, H.-T. Chen, and J. E. Subotnik, arXiv:1812.03265 [physics] (2018), arXiv: 1812.03265.

[35] J. C. Tully, The Journal of Chemical Physics **93**, 1061 (1990).

[36] M. Ben-Nun, J. Quenneville, and T. J. Martínez, J. Phys. Chem. A **104**, 5161 (2000).

[37] T. E. Li, H.-T. Chen, A. Nitzan, M. Sukharev, and J. E. Subotnik, The Journal of Physical Chemistry Letters **9**, 5955 (2018).

[38] B. Renaud, R. M. Whitley, and C. R. Stroud, Journal of Physics B: Atomic and Molecular Physics **10**, 19 (1977).

[39] The fraction of the coherent component also depends on the incident field intensity. As shown in Ref. 34, the Ehrenfest+R results and analytical calculations based on the quantum OBE are in quantitative agreement.

[40] D. E. Browne and C. H. Keitel, Journal of Modern Optics **47**, 1307 (2000).

[41] Y. Yan, Z. Lü, and H. Zheng, Physical Review A **88** (2013), 10.1103/PhysRevA.88.053821.

[42] R.-C. Ge, S. Weiler, A. Ulhaq, S. M. Ulrich, M. Jetter, P. Michler, and S. Hughes, Optics Letters **38**, 1691 (2013).

[43] A. Laucht, S. Simmons, R. Kalra, G. Tosi, J. P. Dehollain, J. T. Muhonen, S. Freer, F. E. Hudson, K. M. Itoh, D. N. Jamieson, J. C. McCallum, A. S. Dzurak, and A. Morello, Physical Review B **94** (2016), 10.1103/PhysRevB.94.161302.

[44] W. H. Miller, The Journal of Chemical Physics **136**, 210901 (2012).

[45] T. Fiedlschuster, J. Handt, E. K. U. Gross, and R. Schmidt, Phys. Rev. A **95**, 063424 (2017).

[46] A. Castro, A. Rubio, and E. K. U. Gross, The European Physical Journal B **88** (2015), 10.1140/epjb/e2015-50620-1.

[47] A. Schild and E. K. U. Gross, Physical Review Letters **118** (2017), 10.1103/PhysRevLett.118.163202.

[48] S. J. Cotton and W. H. Miller, The Journal of Chemical Physics **139**, 234112 (2013).

- [49] A. Salam, *Atoms* **6**, 56 (2018).
- [50] F. C. Spano and S. Mukamel, *The Journal of Chemical Physics* **91**, 683 (1989).
- [51] S.-H. Lim, T. G. Bjorklund, F. C. Spano, and C. J. Bardeen, *Physical Review Letters* **92** (2004), 10.1103/PhysRevLett.92.107402.
- [52] F. C. Spano, *Accounts of Chemical Research* **43**, 429 (2010).
- [53] N. M. Hoffmann, H. Appel, A. Rubio, and N. T. Maitra, *The European Physical Journal B* **91** (2018), 10.1140/epjb/e2018-90177-6.
- [54] R. F. Ribeiro, L. A. Martínez-Martínez, M. Du, J. Campos-Gonzalez-Angulo, and J. Yuen-Zhou, *Chemical Science* **9**, 6325 (2018).
- [55] L. A. Martínez-Martínez, R. F. Ribeiro, J. Campos-González-Angulo, and J. Yuen-Zhou, *ACS Photonics* **5**, 167 (2018).
- [56] M. Sukharev and A. Nitzan, *J. Phys.: Condens. Matter* **29**, 443003 (2017).